Plant Physiology and Biochemistry 139 (2019) 102–112

Contents lists available at ScienceDirect

Plant Physiology and Biochemistry

journal homepage: www.elsevier.com/locate/plaphy

Research article

Comparative analyses of cuticular waxes on various organs of faba bean (*Vicia faba* L.)

Xiao Zhao[a], Lei Huang[a], Lin Kang[a], Reinhard Jetter[b], Luhua Yao[a], Yang Li[a], Yu Xiao[a], Dengke Wang[a], Qianlin Xiao[a], Yu Ni[a], Yanjun Guo[a,*]

[a] College of Agronomy and Biotechnology, Southwest University, Chongqing, 400716, China
[b] Department of Botany, University of British Columbia, 6270 University Boulevard, Vancouver, BC V6T 1Z4, Canada

ARTICLE INFO

Keywords:
Biosynthesis
Chain length distribution
Cuticular wax
Petals
Wax esters
Vicia faba (faba bean)

ABSTRACT

Cuticular waxes cover the plant surface and serve as hydrophobic layer, exhibiting various wax profiles between plant species and plant organs. This paper reports comprehensive analysis of the waxes on organs exposed to air, including leaf, stem, pod pericarp, and petals (banner, wing and keel), and on seed coat enwrapped in pod pericarp of faba bean (*Vicia faba*). In total 7 classes of wax compounds were identified, including fatty acids, primary alcohols, alkyl esters, aldehydes, alkanes, cinnamyl alcohol esters, and alkylresorcinols. Overall, primary alcohols dominated the waxes on leaves and the seed coat enwrapped in pod pericarp, alkanes accumulated largely in stem and petals, whereas alkylresorcinols were observed in leaf, stem and pod pericarp. Organs exposed to air had higher coverage ($> 1.2\,\mu g/cm^2$) than those on seed coat ($< 0.8\,\mu g/cm^2$), and keel having the highest wax coverage. Meanwhile, the wax coverage on seed coat reduced during the seed development. The variations of wax coverages, compound class distributions and chain length profiles among organs suggested that wax depositions were associated with their ecophysiological functions, and the enzymes involved in wax biosynthesis also showed organ-specific.

1. Introduction

During the evolution of land plants from a relative aquatic environments such as green algae, to a dry environments such as complex gymnosperms and angiosperms (Harholt et al., 2016), the appearance of cuticle on outermost of the land plants was one of the most successful evolutionary products (Riederer, 1991). The plant cuticle is an extracellular hydrophobic layer that covers the aerial epidermis of all land plants, providing protection against desiccation and external environmental stresses (Yeats and Rose, 2013). Crops, after million years of evolution and frequent human selection, are mainly grown on land. Their harvest is mainly relying on rainfall and irrigation in most regions. However, the frequent changes of climate all over the world make crop production unsustainable (Purola et al., 2018). The abilities of crop in adapting to changing environments such as drought and high temperature will reduce the exterior energy investments in improving the crop adaptation and productivity (Prato et al., 2010; Webber et al., 2014).

The cuticles are consisted of cutin and cuticular wax. The former is a polymer mainly consisting of ω- and mid-chain hydroxy or epoxy C_{16} and C_{18} fatty acids and glycerol (Graça and Lamosa, 2010), whereas the cuticular waxes include the epicuticular wax covering on the cutin surface and the intracuticular wax embedded within the cutin matrix (Jetter et al., 2006). Though plant species differ in their wax chemical profiles, the basic wax compounds identified in most plant species are similar, consisting mostly of homologous series of hydrocarbons, wax esters, aldehydes, alcohols and fatty acids. In some plants, specific compounds were identified, such as β-diketone in wheat (*Triticum aestivum* L.) (Wang et al., 2015), and alkylresorcinols in rye (*Secale cereale*) (Ji and Jetter, 2008). In some plants, scanning electron microscope reveals that the epicuticular wax could form crystalloids (Barthlott et al., 1998). *Liriodendron* leaves have surface crystalloids in

Abbreviations: BSTFA, bis-N,O-trimethylsilyltrifluoroacetamide; ER, endoplasmic reticulum; FID, flame ionization detection; G3P, glycerol-3-phosphate; GPAT, glycerol-3-phosphate acyltransferase; GC, gas chromatography; FHT, omega-hydroxy fatty acid/fatty alcohol hydroxycinnamoyl transferase; KCS, 3-ketoacyl-CoA synthase; KCR, ketoacyl-CoA reductase; HCD, hydroxyacyl-CoA dehydratase; ECR, enoyl-CoA reductase; MAG, monoacylglyceride; MAH, mid-chain alkane hydroxylase; MS, mass spectrometry; PKS, polyketide synthase; TAG, triacylglyceride; VLCFA, very long chain fatty acid; FAE, fatty acid elongase; SEM, scanning electron microscopy

* Corresponding author.
E-mail address: qhgyj@swu.edu.cn (Y. Guo).

https://doi.org/10.1016/j.plaphy.2019.03.015
Received 15 January 2019; Received in revised form 8 March 2019; Accepted 8 March 2019
Available online 12 March 2019

the shape of transversally ridged rodlets formed by hentriacontan-16-one, Tilia leaves show quandrangular rodlets formed by beta-amyrenyl acetate, while *Quercus* has fringed edged platelets formed by tetracosanol (Gulz, 1994). Studies have shown that chemical profiles of leaf cuticular waxes will alter with the changes of environmental conditions to improve their adaptations. For example, under drought stress, the cuticular transpiration rate of drought resistant oat variety was most strongly reduced and showed the largest increase in amount of epicuticular wax (Bengston et al., 1978). Water deficit led to the increases in cuticular wax amount per unit area of *Arabidopsis thaliana*, particularly the increases in wax alkanes (Kosma et al., 2009). Leaves with wax absorbed more UV than leaves with little wax, suggesting that the epicuticular waxy layer acts as an ultraviolet radiation protectant in maize (Long et al., 2003). However, due to the significant difference in wax amounts and compositions among plant species (Jetter et al., 2006), wax amounts cannot be used to evaluate the stress resistance between different plant species, suggesting that the wax profile of each plant species has their own mechanism in matching with their adaptations to changing environments.

Organs of crops are mainly divided into two parts, vegetative organs such as leaf, stem and root, and reproductive organs such as flower and seeds. Studies have shown that the chemical profiles covering these organs are different. In potato (*Solanum tuberosum*), total wax coverages vary between petals, leaves, and stems, with stem and leaf dominated by *n*-alkanes and petals dominated with 2-methylalkanes and 3-methylalkanes (Guo and Jetter, 2017). In wheat (*T. aestivum* L.), C_{28} alcohol is the dominant chain length in leaf waxes, whereas C_{24} or C_{26} alcohol was the dominant chain length in spikes depending on varieties (Wang et al., 2015). In maize (*Zea mays*), leaf waxes are mainly primary alcohols and aldehydes, whereas the normal hydrocarbons that occur on silks are part of a homologous series of alkanes, alkenes and dienes of odd-number carbon atoms (Perera et al., 2010). Besides these, the waxes of few crop species have been investigated systematically to date, excepting the leaf wax mixtures of various Brassica cultivars (Lee and Suh, 2015), the waxes on *Rosaceae* fruits such as apple, pear and cherry (Hunsche and Noga, 2011; Verardo et al., 2003; Yin et al., 2011), and the waxes in growing barley (*Hordeum vulgare* L.) leaves (Richardson et al., 2005). For legume crops, even less attention has been paid to investigate their wax profiles systematically, notable exceptions including leaf waxes on alfalfa (*Medicago sativa*) (Ni et al., 2012), pea (*Pisum sativum*) (Sanchez et al., 2001), soybean (Glycine max) (Palacios et al., 2015), and peanut (*Arachis hypogaea*) (Yang et al., 1993). Comprehensive analyses of the wax mixtures coating different organs of legume crops are missing to date. Therefore, it is currently not possible to address the genetic and biochemical mechanisms determining wax composition among different legume organs, then to inform targeted breeding approaches to modify wax composition and enhance legume crop performance.

Forming flower is one of the most important evolutionary products for legume crops to be harvested for grain. During the co-evolution of plant and pollinator insects, the legume flower produces floral fragrance and exhibits colors, shapes and contrasting sizes, to attract pollinators such as bees. The yield and number of mature pods will increase with increased pollination intensity in most legume crops (Groeneveld et al., 2010). A wide diversity of secretory structures such as phenolic cells and tissues, mucilaginous cells, secretory cavities, secretory trichomes and colleters are observed in developing flower petals, exhibiting variation in morphology and location in the flower depending on the species (De Barros et al., 2017). The scent glands are distributed in a restricted way in *Caesalpinia pulcherrima* and *Anadenanthera peregina*, whereas in a diffuse way in *Bauhinia rufa* and *Hymenaea courbaril* (Marinho et al., 2014). These results suggested that the ability of petals in secreting fragrance might differ between locations. The petals of legume crop such as faba bean (*Vicia faba* L.), is mainly consisting of the banner (the uppermost petal), the wings (the narrowed base of the petal), and the keel (the lowermost two petals). The wings serve as a landing platform for a potential pollinator, while the sexual parts of the flower are contained within the keel. The outermost surface of the petal cuticle, and hence the layer are most directly involved in plant-insect interactions (Jeffree, 2006). If these petals were differ in their abilities of fragrance secretion, the chemical profiles of cuticular waxes on these petals might also be different, and the mechanism is still not clear.

Cuticular wax biosynthesis begins with the elongation of long-chain fatty acyl precursors by fatty acyl elongase (FAE) complexes to VLC fatty acyl-CoAs in epidermal plastids (Samuels et al., 2008). Then these VLC fatty acyl-CoAs are exported to the endoplasmic reticulum, where they are catalyzed by cycles of four FAE complexes comprising a ketoacyl-CoA synthase (KCS), a ketoacyl-CoA reductase (KCR), a hydroxyacyl-CoA dehydratase (HCD) and an enoyl-CoA reductase (ECR), finally forming VLC acyl-CoAs with even total carbon number (Haslam et al., 2012; Kunst and Samuels, 2009). Thereafter, two wax biosynthesis pathways are generally involved in most plant species, alcohol forming pathway and alkane forming pathway. In alcohol forming pathway, the acyl-CoAs resulting from FAE elongation are reduced to alcohols, and then the alcohols are esterified with free fatty acids to form alky esters. In alkane forming pathway, the acyl-CoAs resulting from FAE elongation are reduced to aldehydes, and then the aldehydes decarbonylated to alkanes. Meanwhile, the alkanes are further oxidized to secondary alcohols and ketones in some plant species. The identifications of β-diketones on several *Poaceae* have been proven that these compounds are catalyzed by type III polyketide synthases (PKSs) (Kosma and Rowland, 2016), another wax biosynthesis pathway. In a recent review, Busta and Jetter (2017) also conclude that waxes with secondary functional groups might differ in their biosynthesis at least in part from the ubiquitous wax compounds with which they co-occur. Therefore, detailed investigation on cuticular waxes covering on more plant species and different plant organs will increase our knowledge in understanding wax biosynthesis.

To fill the gap in our understanding of the cuticle chemistry among organs of legume crop and to lay the foundation for wax biosynthesis study, the current study aimed to provide comprehensive qualitative and quantitative analyses of the cuticular waxes on all major organs of faba bean (*Vicia faba* L), an annual legume grown world-wide as a protein source for food and feed. To this end, waxes were sampled from mature leaves, stems, petals (banners, wings, and keels), pod pericarps, and seed coats enwrapped in pod pericarp in different developing stages, from two faba bean cultivars (Chenghu 10 and Sucan 2). The comparisons between the organ waxes and their potential wax biosynthesis pathway were further investigated, aiming to provide basic knowledge in improving legume crop adaptations to adverse stresses through cuticular wax.

2. Materials and methods

2.1. Plant materials and sample preparation

Seeds of faba beans (*Vicia faba* L) were sowed in fields at Beibei Research Station of Southwest University (29°49′N, 106°25′E), located in Chongqing, China, in mid-October 2017. The area has a mean temperature of 17.8 °C and a mean annual rainfall of 1100 mm during the last 30 years. The average daily minimum temperature was 8 °C in December 2017 and the highest temperature was 24 °C in April 2018. The soil was a neutral yellow soil with soil pH 7.8, alkali-dispelled nitrogen 75.32 mg/kg, available phosphorus (Olsen-P) 11.45 mg/kg, and available potassium 50.65 mg/kg. Before sowing, the soil was applied with 80 kg N, 80 kg P_2O_5 and 40 kg K_2O per hectare. The fields were randomly separated into four plots with the area of each plot reached 30 m^2 (5 m × 6 m). Each plot was further separated into two subplots (2 m × 6 m). Two cultivars of faba bean (Chenghu 10 and Sucan 2) were separately sown in two subplots of each plot with 30 cm between rows and 15 cm between plants. The crop was weeded two

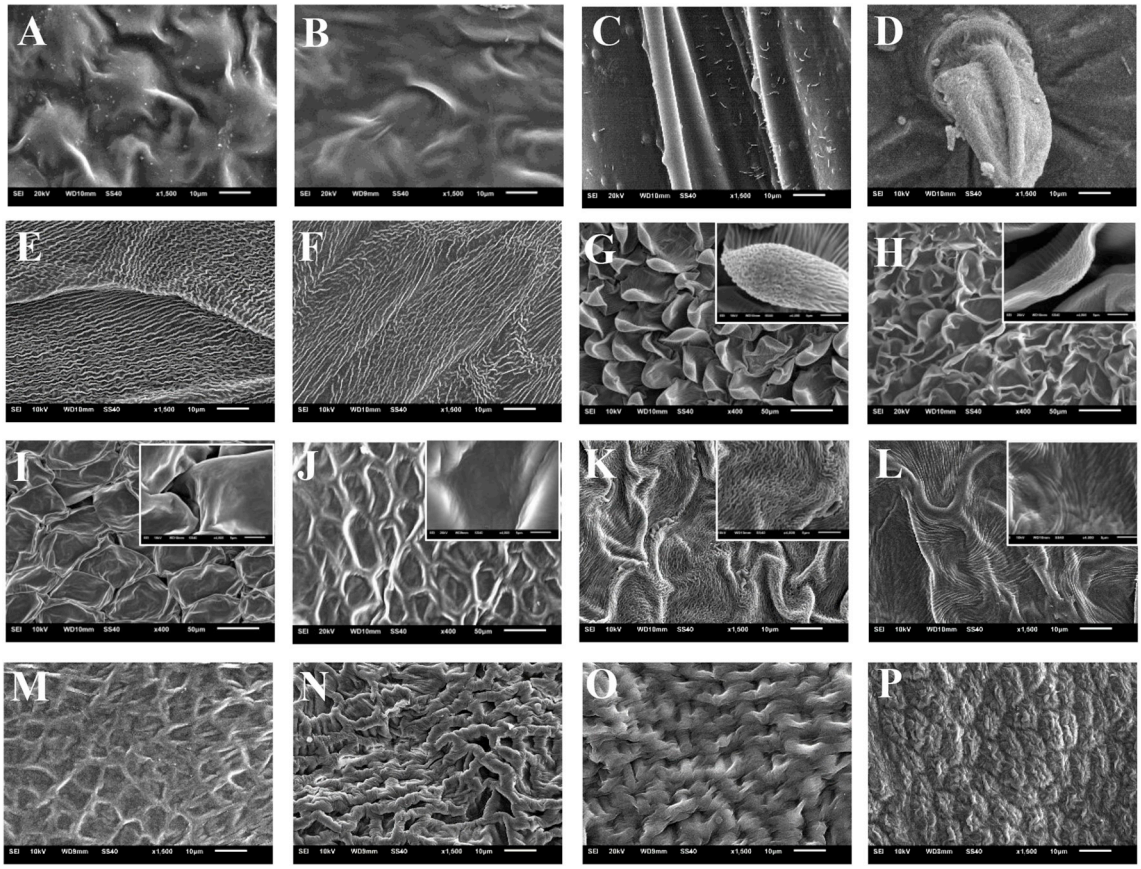

Fig. 1. Scanning electron micrographs of cuticular surfaces on various organs of Faba bean (Suocan 2). A, adaxial side of the leaf; B, abaxial side of the leaf; C, stem; D, pod pericarp; E, adaxial side of the banner petal; F, abaxial side of the banner petal; G, adaxial side of the wing petal (eye region); H, abaxial side of the wing petal (eye region); I, adaxial side of the wing petal (region surrounding the eye); J, abaxial side of the wing petal (region surrounding the eye); K, adaxial side of the keel petal; L, abaxial side of the keel petal; M, seed coat (W1 stage); N, seed coat (W2 stage); O, seed coat (W stage3); P, seed coat (W4 stage). Seed coats in the W1, W2, W3 and W4 stages were harvested three, four, five and six weeks after bloom, respectively. Scale bars in A, B, C, D, E, F, K, L, M, N, O, P: 10 μm; G, H, I, J: 50 μm; inserts: 5 μm.

times (December and February). No irrigation, fertilization or herbicide was applied during the growing period. Four subplots from four plots were regarded as four replicates for each cultivar.

Plant samples were collected in March 2018 when most plants were in their blossom stages. Leaves, stems and petals were sampled from five plants in each subplot for each cultivar. The third expanded leaf from top of the main stem was collected; the main stem between the third leaf and the fifth leaf from the top was collected. Petals were sampled with tweezers, and then manually divided into banners, wings and keels. Three flowers were collected from each plant. For samples of seed coat, 10 flowers in each plant and 20 plants in each subplot were marked after blossoming, and then two pods were collected from two plants in each subplot at each sampling time. Pods were sampled four times in total, one three weeks after blossom, then once every one week. The beans could be separated from the pod three weeks after blossom. Six weeks after blossom, the beans were ready for harvest for fresh beans. Two whole pods were used for wax extraction from its pod pericarp in each subplot for each cultivar. All samples from same cultivar in each subplot were mixed together before wax extraction, and then used immediately for wax extraction.

2.2. Wax extraction

Before wax extraction, photos of leaves, stems, petals and pod pericarps were taken and subjected to pixel counting using the ImageJ software to determine surface areas (Abramoff et al., 2004). The beans were approximately cuboid. Therefore, the length, width and height were measured separately with a vernier caliper (precision 0.02 mm), and then used to calculate the surface area of seed coat using the following equation.

$$\text{Surface area } (cm^2) = 2 \times (\text{length} \times \text{width} + \text{length} \times \text{height} + \text{width} \times \text{height})$$

Then, the surface wax mixtures were extracted twice for 30 s with $CHCl_3$. The two extracts from each sample were then combined and filtered through glass wool, and the solvent was evaporated under N_2. *n*-Tetracosane was added to the fresh plant material before extraction, 5 μg for leaves, stems, banners, wings, keels and pod pericarps, and 2 μg for seed coats.

2.3. Wax sample preparation and GC analysis

Wax samples were prepared for GC analysis by dissolving them in pyridine (50 μL, Aldrich), then adding bis-N,O-trimethylsilyltrifluoroacetamide (BSTFA, 50 μL, Aldrich). Mixtures were incubated at 70 °C for 45 min, then excess reagents were evaporated under N_2, and $CHCl_3$ (500 μL) was finally added.

For compound identification, the GC analysis was carried out with 9790II gas chromatograph (Fu-Li, China). The GC column was DM-5 capillary column (30 m × 0.32 mm × 0.25 μm). Nitrogen was served as the carrier gas. The GC oven was held at 80 °C for 10 min, heated at 5 °C/min to 260 °C, where the temperature remained 10 min. The temperature was then heated at 2 °C/min to 290 °C, and further heated at 5 °C/min to 320 °C, where the temperature was held for 10 min.

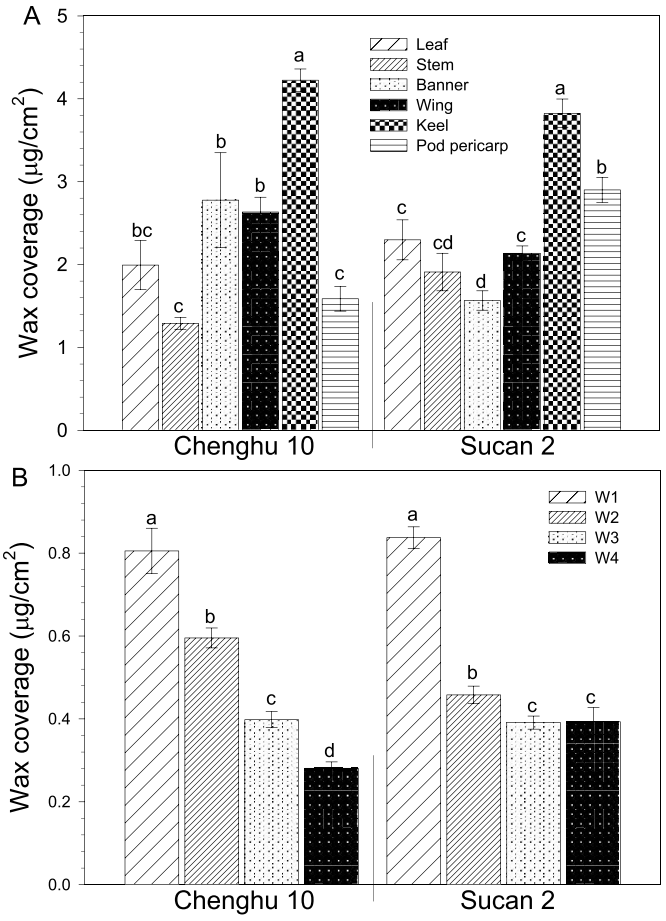

Fig. 2. Wax coverages on the surfaces of various organs of two varieties of *Vicia faba* L:(A) aerial organs; (B) seed coat. Data are given as averages of four biological replicates with standard errors. Different letters above the bars indicate significant differences between respective organs according to Tukey's HSD tests ($P < 0.05$).

Compounds were detected with a GCMS-QP2010 Ultra Mass Spectrometric Detector (Shimadzu Corp., Kyoto, Japan) using HP-5 MS capillary column (30 m × 0.32 mm × 0.25 μm), and He as the carrier gas. Compounds were identified by comparing their mass spectra with published data and authentic standards.

Alkyl resorcinol homologs were identified based on characteristic fragment combinations m/z 268 (100) and 281, together with respective molecular ions m/z 492 (M-15 = 477), 506 (M-15 = 491), 520 (M-15 = 505), 534 (M-15 = 519), 548 (M-15 = 533), 562 (M-15 = 549), and 576 (M-15 = 561) (Luna, 2014). Cinnamyl alcohol ester homologs were identified based on characteristic fragment combinations m/z 43, 57, 71, 85, 117 (100), 133, 267 (C18), 295 (C20), 323 (C22), and 351 (C24), together with respective molecular ions m/z 400, 428, 456, and 484 (Griffiths et al., 1999). Alkyl ester homologs were identified based on characteristic fragment combinations m/z 57, 71, 85, 285, 313, 341, 369 and 397, together with respective molecular ions m/z 620 (C42), 648 (C44) and 676 (C46) (Gülz et al., 1993).

Compounds were quantified by GC coupled to a flame ionization detector (FID) set at 250 °C, burning H_2 (30 mL/min) in air (200 mL/min), with the flame shaped by N_2 (20 mL/min). Wax compound peak areas were compared against the internal standard peak area for quantification. The relative response factors relative to the internal standard were taken as 1.00 for all cuticular wax constituents regardless of chain length and compound class, in agreement with past reports using the same GC conditions (Riederer and Schneider, 1989).

2.4. Scanning electron microscopy

To examine the morphology of epicuticular wax by scanning electron microscopy (SEM), fresh leaf, stem, pod pericarp, petals, and seed coats were carefully collected, rinsed thoroughly with distilled water to get rid of dust, air dried, and then affixed to an aluminum stub with double-sided adhesive tape. The plant samples were coated with Au and then viewed by SEM (Hitachi S3500 and JSM-6510LV).

2.5. Statistical analysis

Data are presented as the means ± standard error of four independent samples. One-way ANOVA was used to compare the difference of total wax coverage among organs (SPSS 17.0, USA). The differences between means were evaluated using Tukey HSD tests. Statistical significance was considered at $P < 0.05$.

3. Results and discussion

The present work aimed to provide a comprehensive characterization of all major above-ground organ surfaces of *V. faba*, using scanning electron microscopy (SEM) to visualize their micro-relief, gas chromatography (GC) coupled with mass spectrometry (MS) to identify components of the cuticular wax mixtures present, and GC with flame ionization detection (FID) to quantify the overall amounts of waxes, the compound classes comprising them, and the chain length and isomer profiles within them.

3.1. Surface wax micro-relief

Detailed SEM studies revealed the micro-relief on the vegetative above-ground organs of faba bean. The adaxial and abaxial leaf surfaces showed only gentle undulation of epidermal cells, and mostly smooth wax films covering the cells (Fig. 1 A, B). Only very few, small wax crystals were detected, exclusively on the adaxial leaf surface (Fig. 1 A). The stem surfaces exhibited cellular folds running parallel to the shoot axis, and a few wax platelets protruding from the smooth wax film (Fig. 1 C). Pod pericarps had pavement cells as well as trichomes, both covered by wax films with small granules (Fig. 1 D).

The surface micro-relief also varied greatly between different types of petals and regions on them. Both the adaxial and the abaxial sides of the banner petal had gently undulating cell topographies, with prominent wavy ridges running mostly parallel on them (Fig. 1E and F). The epidermal cells within the black spot, the eye, on the adaxial side of wing petals were highly lobed, with arrays of small ridges lining both the outermost humps of the lobes and their flanks (Fig. 1G). The nearby adaxial surface surrounding the eye had thinner epidermal lobes with only very small, shallow ridges (Fig. 1H). The abaxial sides of the wing petal, both within the eye region and surrounding it, exhibited overall flat surfaces with fairly smooth wax films, and local depressions likely due to shrinkage of underlying epidermal cells during sample preparation (Fig. 1I and J). Both the adaxial and the abaxial sides of the keel petal had relatively smooth surfaces, with arrays of minor ridges (Fig. 1K and L). The seed coat surfaces were fairly smooth in stage 1 (W1) (Fig. 1M), developing more pronounced twisted-rope-like structures formed in stage 2 (W2) and 3 (W3) (Fig. 1N, O), and undulating relief with granular fine-structure in stage 4 (W4) (Fig. 1P). Wax crystals were not observed on any of the petal or seed coat surfaces. The Suocan 2 cultivar showed surface micro-reliefs on all organs very similar to those of cv Chenghu 10.

Papillae and cuticular folds are characteristic structures of many epidermal surfaces (Christensen and Hansen, 1998; Koch et al., 2013), and they are known to greatly affect surface wettability and self-cleaning (Barthlott et al., 1998; Koch and Ensikat, 2008). Here, we found that the surfaces of faba bean petals are lined by epidermal cells exhibiting very prominent three-dimensional structures on two

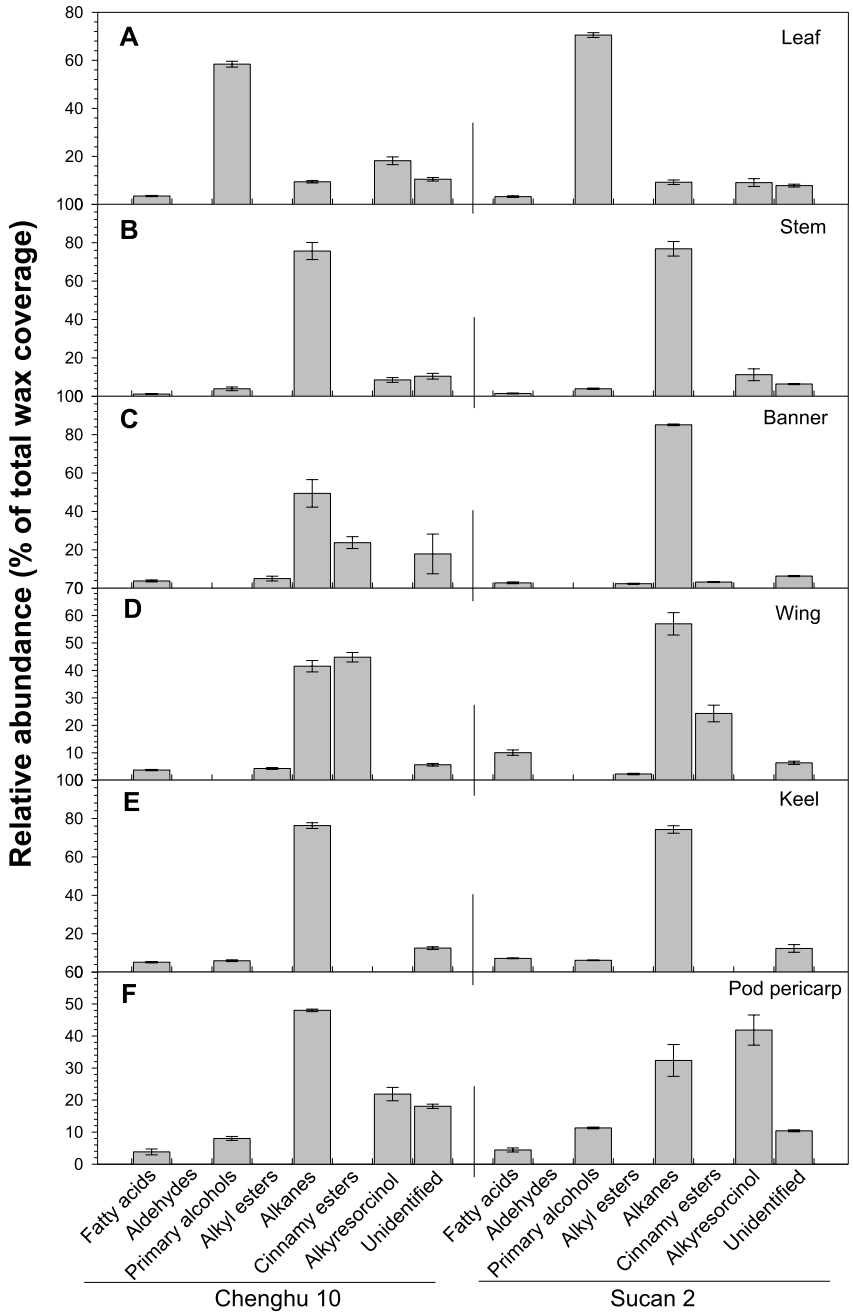

Fig. 3. Wax amount of compound classes covering various organs of Chenghu 10 and Sucan 2: (A) leaf; (B) stem; (C) banner; (D) wing; (E) keel; (F) pod pericarp. Data are given as averages of four biological replicates with standard errors.

different length scales, combining cellular lobes and cuticular ridges. Together, these features will have substantial effects on reflection of visible light and ultraviolet radiation, thus impacting the macroscopic appearance of the tissue and its effect on pollinators (Whitney et al., 2009). In this context it is interesting to note that micro-rough surfaces featuring ridges and lobes similar to those on faba bean petals may provide footholds for flies and honeybees (Brauer et al. (2017). In contrast, flat epidermal cells covered with nano-scale epicuticular wax crystals would impair attachment, however such smaller surface features were absent from the petal surfaces.

3.2. Wax coverage

To provide a comprehensive analysis of the cuticular wax mixtures covering each of the above-ground faba bean organs, we determined the absolute quantities of the mixtures overall (in μg/cm^2) and the relative contributions of compound classes, chain lengths and isomers within them (in %). The total wax coverages varied relatively little between cultivars, but substantially between organs within each cultivar (Fig. 2A). Leaves and stems had moderate wax coverages of 1.99 μg/cm^2 and 1.29 μg/cm^2 in cv. Chenghu 10, respectively, and 2.29 μg/cm^2 and 1.91 μg/cm^2 in cv. Sucan 2. Petal surfaces had highly varying apparent wax coverages, with 2.78 μg/cm^2, 2.63 μg/cm^2 and 4.22 μg/cm^2 on banners, wings and keels of cv. Chenghu 10, respectively; and 1.57 μg/cm^2, 2.14 μg/cm^2 and 3.82 μg/cm^2 for cv. Sucan 2, respectively.

It should be noted that petal wax coverages were determined relative to macroscopic surface areas, without taking microscopic topography into account. The true coverages are likely lower where epidermal cells had undulating surfaces or even lobes protruding, and the

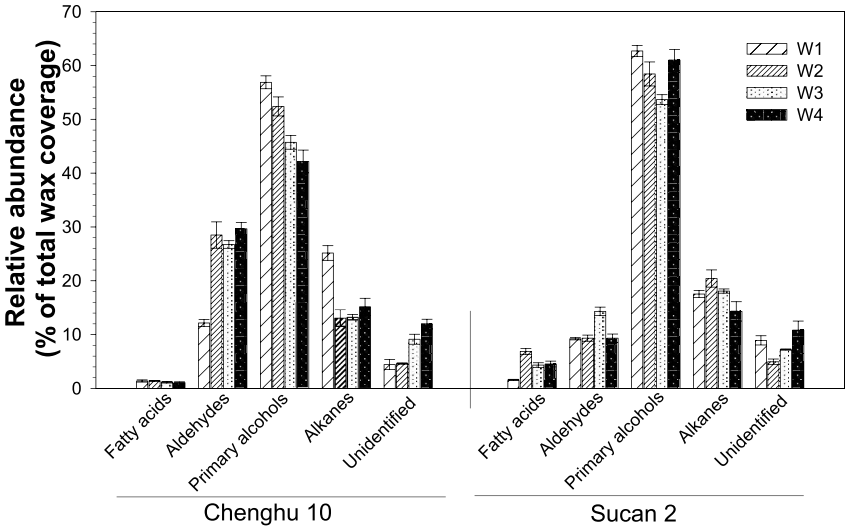

Fig. 4. Compound class profiles of wax mixtures in four developmental stages of *Vicia faba* seed coats. Data are given for the cultivars Chenghu 10 and Sucan 2 as averages of four biological replicates with standard errors. Starting three weeks post-anthesis (18 weeks after sprouting), pods were sampled every seven days for seed coat wax extraction. W1 seed coat wax three weeks post-anthesis; W2 seed coat wax four weeks post-anthesis; W3 seed coat wax five weeks post-anthesis; W4 seed coat wax six weeks post-anthesis.

wax coverage values given here must therefore be taken as upper limits for the true, local wax amounts. The wax coverages reported here are intermediate between those of many other species and organs. For dandelion (*Taraxacum officinale*) petals, a total wax coverage of 36.95 μg/cm^2 was reported, which was circa five times higher than the coverage of leaves in the same species (Guo et al., 2017). In contrast, *Cosmos bipinnatus* petals had total wax loads of 2.7 μg cm^{-2} and thus about a fifth of the leaf wax coverages (Buschhaus et al., 2015).

The seed coats of both cultivars had very similar wax coverages, which were steadily declining during seed coat development (Fig. 2 B). Overall, wax coverage reduced by 37% in cv. Chenghu 10 and 49% in cv. Sucan 2 from the W1 stage (two weeks after flowering) to the W4 stage (five weeks after flowering). In the same period, the seed coat surface areas increased by 235% in Chenghu 10 and 528% in Sucan 2 (data not shown), and the decrease in wax coverages during seed development is therefore largely due to surface expansion. However, the finding that the decrease in wax coverage was much less than the increase in surface areas suggests substantial accumulation of newly formed wax throughout seed coat development, to largely (but not entirely) compensate for surface growth. This result is similar to previous reports on wax coverages during organ development, where for example pavement cells on *Arabidopsis* leaves maintained constant wax coverages during leaf growth, indicating that wax accumulation may be synchronized with cell expansion throughout tissue development (Busta et al. (2017).

Wax **C**lass **C**omposition. Up to date, no cuticular wax data on faba bean was available in reported resources, excepting for analysis of epicuticular waxes and volatiles on faba bean flowers from a study by Griffiths et al. (1999). Here, seven different classes of compounds were identified within the wax mixtures covering above-ground faba bean organs, including fatty acids, primary alcohols, alkyl esters, aldehydes, alkanes, cinnamyl alcohol esters and alkylresorcinols (Fig. 3). Among them, only alkanes were detected in all organs, with relative amounts of ca. 9% on leaves, 76% on stems of both cultivars, and 45% and 85% on banners, 42% and 57% on wings, 83% and 81% on keels, and 47% and 31% on pod pericarps of cv. Chenghu 10 and cv. Sucan 2, respectively. Small amounts of fatty acids were observed in leaf wax (ca. 3% in both cultivars), stems (ca. 1%), banner petals (ca. 3.5%), wing petals (ca. 7%), keel petals (ca. 5%), pod pericarps (ca. 3.5%) and seed coats (ca. 3%). Primary alcohols dominated the wax mixtures on leaves (ca. 65%) and seed coats (ca. 54%), while being present in smaller amounts on stems (ca. 4%) and pod pericarps (ca. 6%), and not detectable on any of the petal surfaces. Aldehydes were detected only on keels (4.5% across two cultivars) and seed coats (21%). Alkyl esters were detected only on banner (ca. 3.5%) and wing petals (ca. 3%), while cinnamyl alcohol esters were found prominently on banners (22% in cv. Chenghu 10 and 3% in cv. Sucan 2) and wings (45% in cv. Chenghu 10 and 25% in cv. Sucan 2), and alkylresorcinols in leaf (ca. 14% in both cultivars) as well as stem wax (ca. 11%). Less than 10% of the wax mixtures from most organs remained unidentified (except for 13–18% on banners and pod pericarps of cv. Chenghu 10, and keels of both cultivars).

High abundance of alkanes is very common in petal waxes. However, petals varied in their alkane abundance, which might be associated with their physiological functions. For example, higher abundance of alkanes on keel might contribute to its role in protecting pistil from dehydration by changing environments (Lee et al., 2014; Ni et al., 2012). The alkylresorcinols (1,3-dihydroxy-5-n-alk(en)ylbenzenes) detected on leaf and stem, acting as chemical signals, might be involved in the complex plant resistance system (Luis et al., 2016). For example, they were strong growth inhibitors of many fungal species such as *Aspergillus niger* and *Penicillium crysogenum* (Garcia et al., 1997). As member of phenolic lipids, alkylresorcinols are thought to be derived predominantly from type III polyketide synthase (PKS)-associated pathways (Abe and Morita, 2010). The cinnamyl alcohol, naturally presents only in small amount, has a distinctive odour and is mainly used in perfumery (Letizia et al., 2005). It was also detected in flowers of *Mimusops elengi* (Wong and Teng, 1994), *Hyacinthus orientalis* (Hosokawa and Fukunaga, 1995), and *Plumeria rubra* (Pino et al., 1994). However, such compounds are not common in cuticular waxes, partly due to their sensitivity to air, where cinnamyl alcohol readily autoxidizes upon air exposure (Niklasson et al., 2013). In faba bean petals, these esters might serve as attractants for species-specific pollinators, or appear to protect plants by deterring herbivores and by attracting the enemies of herbivores (Pichersky and Gershenzon, 2002). And further investigation is needed to clarify what the direct functions of these esters are in faba bean petals.

Esters, main constitutes of flower volatiles, play important roles in flower-insect interactions (Griffiths et al., 1999; Tava and Pecetti, 1997). Surprisingly, no esters were detected on keel, excepting banner and wing faba bean petals. This suggested that the biosynthesis of volatile esters on petals of Papilionoideae differed among petals, associated with their special functions formed during long-term coevolution between flower and insect (Pellmyr, 1992). Most Papilionoideae species exhibit specialized flowers, with the banner petal placed in the upper position and the keel and flanking wings acting as the landing platform for bee visitors (Amaral-Neto et al., 2015). The keel is formed by two petals that enclose the gynoecium and stamens, blocking the free access to pollen by flower visitors (Westerkamp, 1997). The banner and wings, containing fragrance consisted of esters, might serve as insect pollinator attractor (Marinho et al., 2014).

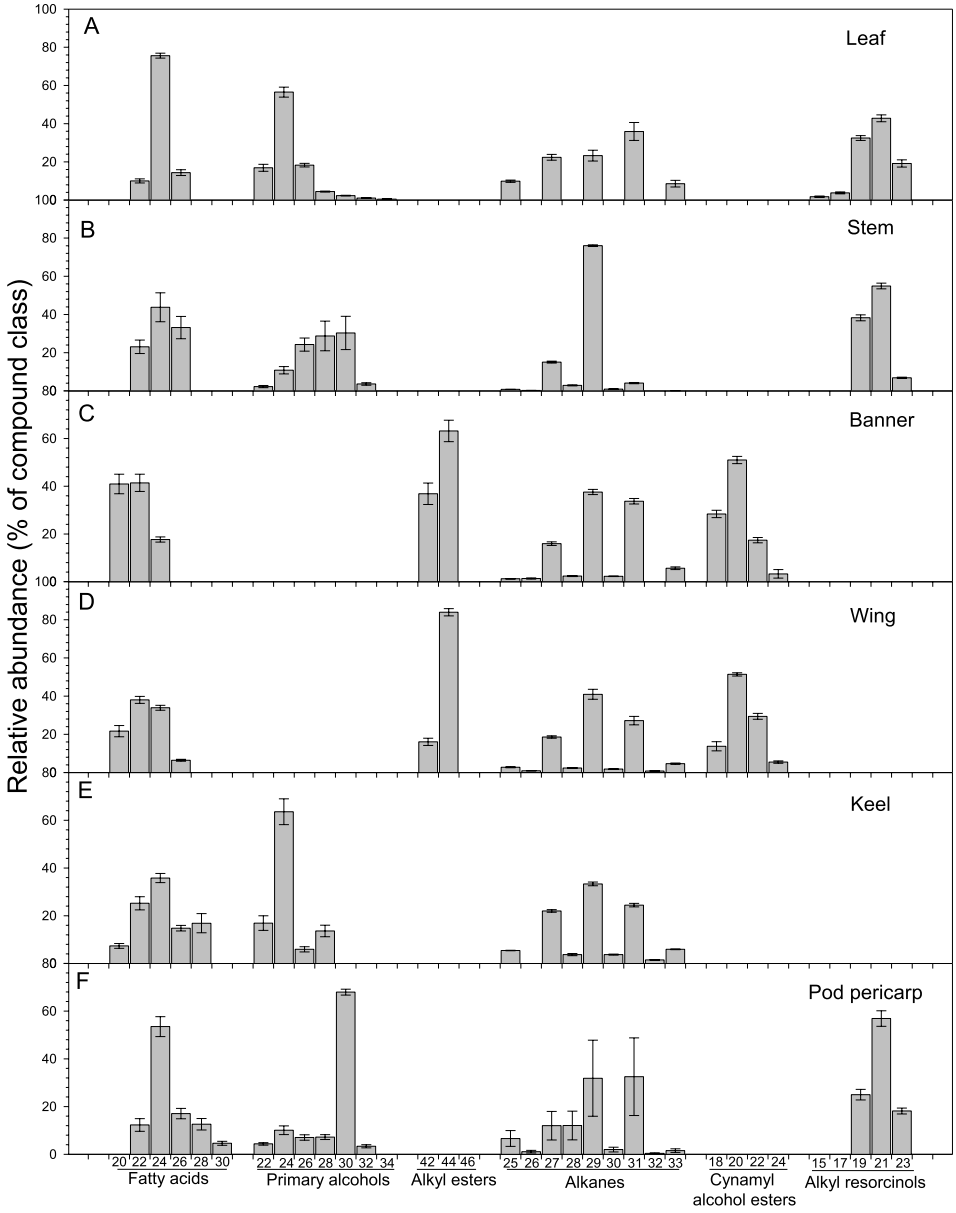

Fig. 5. Chain length distributions within the compound classes in wax mixtures covering various organs of *Vicia faba* cv. Chenghu 10. Relative abundances (% of each compound class) are plotted for fatty acids, primary alcohols, alkyl esters, alkanes, cinnamyl alcohol esters and alkyl resorcinols with aliphatic chain lengths given by the numbers on the x-axis for (A) leaf; (B) stem; (C) banner; (D) wing; (E) keel; (F) pod pericarp. Values are averages of four biological replicates with standard errors. tr, trace amounts.

The wax mixtures on seed coats of both cultivars were dominated by primary alcohols, with steadily decreasing relative amounts in cv. Chenghu 10 but only small variation in cv. Sucan 2 during pod development (Fig. 4). Alkanes amounted to 15–25% of the seed coat wax mixtures in both cultivars, with relatively little change throughout development. The seed coat waxes of cv. Sucan 2 contained relatively constant amounts of aldehydes throughout development (mostly around 29% in cv. Chenghu and 11% in cv. Sucan 2). Fatty acid amounts also varied little, at approximately 2% in cv. Chenghu and 5% in Sucan 2. Between 4% and 12% of the wax mixtures on the seed coats of both cultivars remained unidentified in the different developmental stages.

Our findings on development of seed coat waxes further supported that wax accumulation was synchronized with cell expansion throughout seed coat development (Busta et al., 2017), and the deposition of different wax component was also synchronized and they might balance each other in deposition to keep relatively stable wax compositions. A study with *Hedera helix* also has shown that wax amounts in the apolar fraction reached a maximum first and then gradually decreased again during the remaining period of the season, whereas the polar wax fraction rapidly increased early in the season, reaching a plateau after 40 d, and then remained constant during the rest of the season (Hauke and Schreiber, 1998).

Overall, primary alcohols dominated the waxes on leaves and the seed coat enwrapped in pod pericarp, alkanes accumulated largely in stem and petals, whereas alkylresorcinols were observed in leaf, stem and pod pericarp. Our results thus suggest differential regulation of wax biosynthesis in different faba bean organs, leading to strongly enhanced flux through the alkane-forming pathway in leaf and petals, the alcohol-forming pathways in leaf and seed coat, and type III PKS-associated pathways in leaf, stem and pod pericarp.

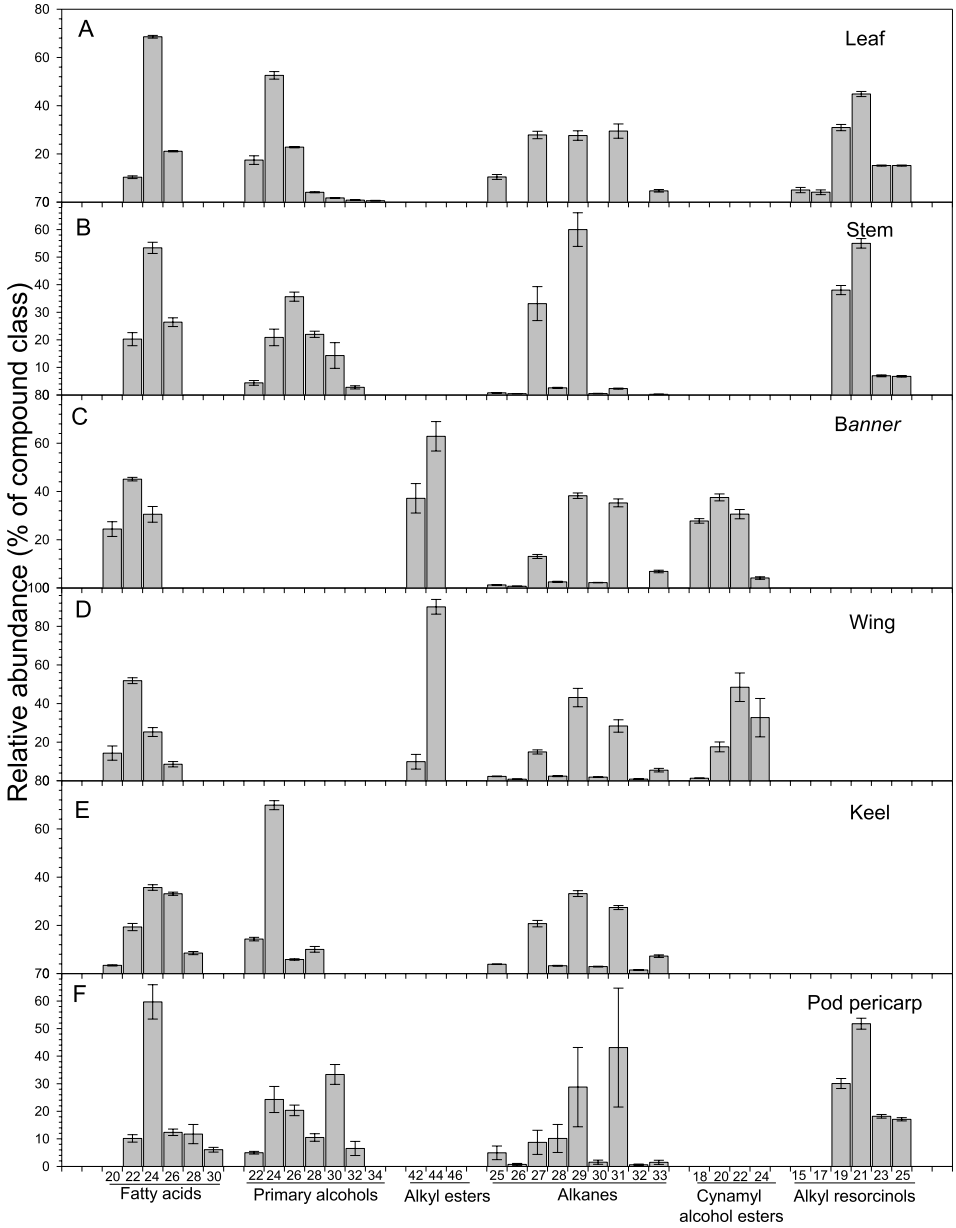

Fig. 6. Chain length distributions within the compound classes in wax mixtures covering various organs of *Vicia faba* cv. Sucan 2. Relative abundances (% of each compound class) are plotted for fatty acids, primary alcohols, alkyl esters, alkanes, cinnamyl alcohol esters and alkyl resorcinols with aliphatic chain lengths given by the numbers on the x-axis for (A) leaf; (B) stem; (C) banner; (D) wing; (E) keel; (F) pod pericarp. Values are averages of four biological replicates with standard errors. tr, trace amounts.

3.3. Chain length distributions within compound classes of faba bean wax mixtures

Within the different compound classes of *V. faba* surface waxes, series homologs with characteristic chain length distributions were found. Fatty acids, primary alcohols and alkyl esters with predominantly even carbon numbers were found, while the alkanes comprised mainly odd-numbered homologs (Fig. 5). In cv. Chenghu 10, fatty acids with chain lengths varying from C_{20} to C_{30} were identified in mixtures strongly dominated by C_{24} acid on leaves and pod pericarps, roughly equal amounts of C_{24} and C_{26} acids on stems and wing petals, and similar levels of C_{22} and C_{24} acids on banner and keel petals. A wide range of primary alcohols with C_{22} − C_{34} chain were detected in *V. faba* waxes, dominated by C_{24} in the mixtures on leaves and keel petals, C_{26} − C_{30} on stems and C_{30} on pod pericarps. C_{42} and C_{44} alkyl esters were found in banner and keel waxes, with the latter compound dominating. A particularly broad range of alkanes was detected, varying in chain lengths from C_{25} to C_{33} and peaking at C_{29} in the waxes of most organs. The chain length profiles of all compound classes on all organs of *V. faba* cv. Sucan 2 closely matched those of cv. Chenghu 10 (Fig. 6).

The only aromatic compound classes detected in *V. faba* waxes were the cinnamyl alcohol esters on banner and wing petals, and the alkylresorcinols on leaves, stems and pod pericarps. The cinnamyl alcohol esters had fatty acid moieties varying in chain lengths from C_{18} to C_{24}, with the C_{20} homolog dominating in the waxes from both petals of both cultivars. The alkylresorcinols had aliphatic side chains with both odd and even numbers of carbons ranging from C_{15} to C_{23} (Figs. 5 and 6). The odd-numbered C_{19}, C_{21} and C_{23} homologs were found to predominate in all three organs of both cultivars.

Though cinnamyl alcohol esters are less reported in cuticular waxes, they play important role in lignin biosynthesis (Kuroda, 2000). For

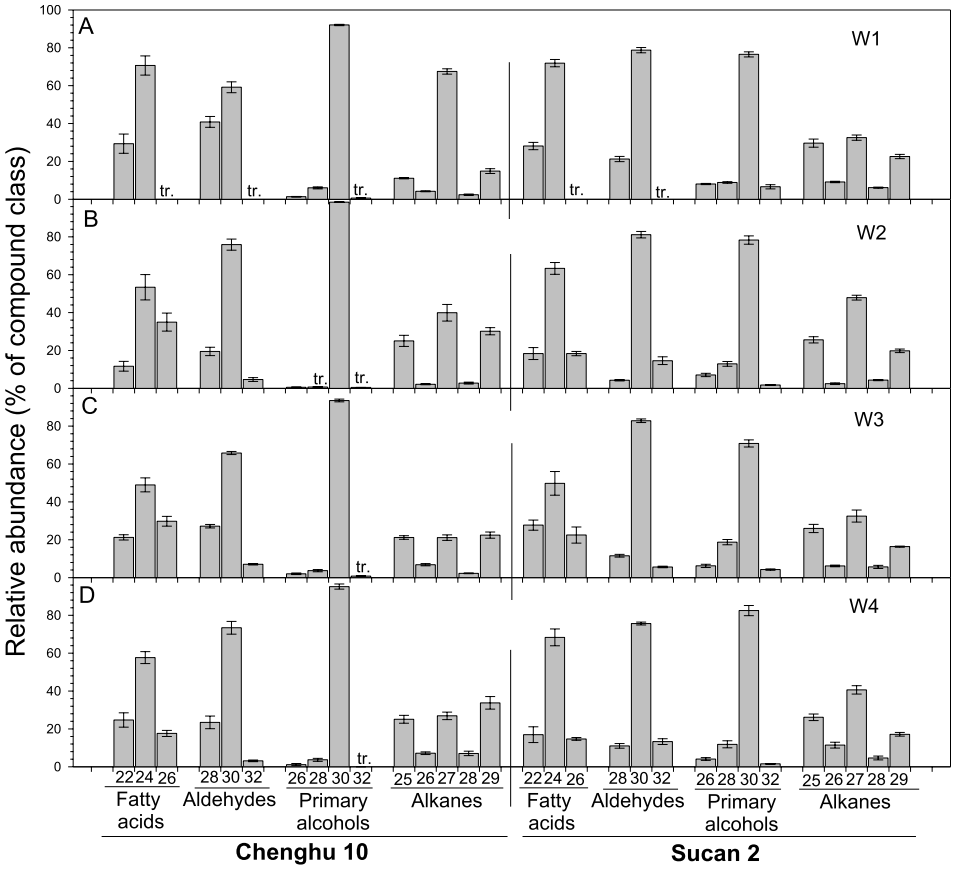

Fig. 7. Chain length distributions within the compound classes in wax mixtures covering seed coats of *Vicia faba* cv. Chenghu 10 and cv. Sucan 2. Relative abundances (% of each compound class) are plotted for fatty acids, aldehydes, primary alcohols and alkanes with aliphatic chain lengths given by the numbers on the x-axis for the seed coat developmental stages (A) W1, (B) W2, (C) W3 and (D) W4. Data are given for the cultivars Chenghu 10 and Sucan 2 as averages of four biological replicates with standard errors. tr, trace amounts.

example, cinnamyl-alcohol dehydrogenase was involved in the control of lignin formation in *Sorghum bicolor* (Pillonel et al., 1991). Overexpression of cinnamyl alcohol dehydrogenase increased lignin in *Artemisia annua* (Ma et al., 2018). Cinnamyl alcohol is also the bioactive component of chestnut flower, inhibiting adipocyte differentiation in 3T3-L1 cells by down-regulating adipogenic transcription factors (Il Hwang et al., 2017). When compared with chain length of alkanes and fatty acids on petals of faba bean, the length of side chain of n-alkylresorcinols was much shorter. This implied that the alkane forming pathway might utilize more long chain fatty acid-CoA, whereas polyketide metabolic pathway utilize more short chain fatty acid-CoA, showing no much competitions on fatty acid-CoAs. The findings of *n*-alkylresorcinols in faba bean also provide an alternative plant material in studying the biosynthesis of cuticular waxes with varying compounds in one plant from alkane forming and alcohol forming pathways to polyketide metabolic pathway.

The seed coat waxes of *V. faba* had chain length profiles overall resembling those of the organs described thus far, but with fewer homologs detectable (Fig. 7). Fatty acids ranging from C_{22} to C_{26} were identified, peaking at C_{24}. The aldehyde and primary alcohol series were strongly dominated by the C_{30} homolog in both cultivars throughout development, while the alkanes comprised substantial amounts of three homologs, C_{25}, C_{27} and C_{29}, in both cultivars and in all developmental stages.

Lower chain length of predominant alkane homolog on seed coat than on the other organs might be correlated with their surrounding environments, suggesting that organs confronting less light exposure and humidity fluctuations might have lower predominant chain length when compared with other aboveground organs. Partly, this might be due to that light affects wax deposition through changes in photon flux density reaching to different organs (Richardson et al., 2005), and thus the expressions of various CER1 alleles involved in the biosynthesis of different chain length alkanes.

4. Conclusion

This study provides detailed epicuticular wax morphologies and comprehensive qualitative and quantitative data on the cuticular waxes on various petals of flower, developing seed coats enwrapped in pod pericarp as well as other aerial organs of faba bean. Our analysis of petal waxes partly confirmed previous reports on faba bean flowers, while firstly reported the compounds class distributions among different petals, such as banners, wings and keels. The keel petal had the highest wax coverage when compared with that on banner and wing petals, predominated by almost 80% of *n*-alkanes. Series of homologs of alkyl esters and cinnamyl alcohol esters were only observed on banner and wing petals, but not on keel petal, showing petal specific. Seed coat had the lowest total wax coverage when compared with other organ exposed to environment, which reduced with the development of seed coat in pod pericarp. Primary alcohols dominated on leaves, whereas *n*-alkanes dominated on stem and pod pericarp. *n*-Alkane was the only one compound class detected on all tested organs, with varying predominant alkane homolog between organs, such as C_{31} on leaf and pod pericarp, C_{29} on stem and petals, and C_{27} on seed coat. *n*-Alkylresorcinols were only observed on leaf, stem and pod pericarp with the long aliphatic chains composed of odd and even numbers of carbons ranging from C_{15} to C_{23}, which were dominated by C_{19}, C_{21} and C_{23} homologs. Faba bean organs varied in their homolog and isomer distributions of various compound classes, which suggested that several wax biosynthesis enzymes with distinct substrate specificities might exist in various organs. Further findings of *n*-alkylresorcinols in faba bean implied that faba bean might be an alternative plant material in studying the biosynthesis of cuticular waxes with varying compounds in one plant from alkane forming and alcohol forming pathways to polyketide metabolic pathway.

Contributions

YG and XZ designed experiments. XZ, LH, LY and YX quantified wax constituent, YJ and RJ identified the wax compounds. LK and DW planted faba bean. YG, XZ, QX, YN and RJ analyzed the data and wrote the manuscript.

Acknowledgments

This research was funded by National Natural Science Foundation of China (31670407, 31771694) and the Fundamental Research Funds for the Central Universities (XDJK2018B021). The authors thank Mr Liangliang Wei and Miss Xiaoting Li for their help with field sampling and GC analysis.

Appendix A. Supplementary data

Supplementary data to this article can be found online at https://doi.org/10.1016/j.plaphy.2019.03.015.

References

Abe, I., Morita, H., 2010. Structure and function of the chalcone synthase superfamily of plant type III polyketide synthases. Nat. Prod. Rep. 27 (6), 809–838.
Abramoff, M., Magelhaes, P., Ram, S., 2004. Image processing wiht ImageJ. Biophot. Int. 11, 36–42.
Amaral-Neto, L.P., Westerkamp, C., Melo, G.A.R., 2015. From keel to inverted keel flowers: functional morphology of "upside down" papilionoid flowers and the behavior of their bee visitors. Plant Systemat. Evol. 301 (9), 2161–2178.
Barthlott, W., Neinhuis, C., Cutler, D., Ditsch, F., Meusel, I., Theisen, I., Wilhelmi, H., 1998. Classification and terminology of plant epicuticular waxes. Bot. J. Linn. Soc. 126 (3), 237–260.
Bengston, C., Larsson, C.S., Liljenberg, C., 1978. Effect of water stress on cuticular transpiration rate and amount and composition of epicuticular wax in seedlings of six oat varieties. Physiol. Plantarum 44, 319–324.
Brauer, P., Neinhuis, C., Voigt, D., 2017. Attachment of honeybees and greenbottle flies to petal surfaces. Arthropod-Plant Interact. 11 (2), 171–192.
Buschhaus, C., Hager, D., Jetter, R., 2015. Wax layers on Cosmos bipinnatus petals contribute unequally to total petal water resistance. Plant Physiol. 167 (1), 80–88.
Busta, L., Hegebarth, D., Kroc, E., Jetter, R., 2017. Changes in cuticular wax coverage and composition on developing Arabidopsis leaves are influenced by wax biosynthesis gene expression levels and trichome density. Planta 245 (2), 297–311.
Busta, L., Jetter, R., 2017. Moving beyond the ubiquitous: the diversity and biosynthesis of specialty compounds in plant cuticular waxes. Phytochemistry Rev. 17 (6), 1275–1304.
Christensen, K., Hansen, H., 1998. SEM-studies of epidermal patterns of petals in the angiosperms. Opera Bot. 135, 1–91.
De Barros, T.C., Marinho, C.R., Pedersoli, G.D., Paulino, J.V., Teixeira, S.P., 2017. Beyond pollination: diversity of secretory structures during flower development in different legume lineages. Acta Bot. Bras. 31 (3), 358–373.
Gülz, P.-G., Markstädter, C., Riederer, M., 1993. Isomeric alkyl esters in Quercus robur leaf cuticular wax. Phytochemistry 35 (1), 79–81.
Garcia, S., Garcia, C., Heinzen, H., Moyna, P., 1997. Chemical basis of the resistance of barley seeds to pathogenic fungi. Phytochemistry 44 (3), 415–418.
Graça, J., Lamosa, P., 2010. Linear and branched poly(omega-hydroxyacid) esters in plant cutins. J. Agric. Food Chem. 58 (17), 9666.
Griffiths, D.W., Robertson, G.W., Shepherd, T., Ramsay, G., 1999. Epicuticular waxes and volatiles from faba bean (Vicia faba) flowers. Phytochemistry 52 (4), 607–612.
Groeneveld, J.H., Tscharntke, T., Moser, G., Clough, Y., 2010. Experimental evidence for stronger cacao yield limitation by pollination than by plant resources. Perspect. Plant Ecol. Evol. Systemat. 12 (3), 183–191.
Gulz, P.G., 1994. Epicuticular leaf waxes in the evolution of the plant kingdom. J. Plant Physiol. 143 (4–5), 453–464.
Guo, Y.J., Busta, L., Jetter, R., 2017. Cuticular wax coverage and composition differ among organs of Taraxacum officinale. Plant Physiol. Biochem. 115, 372–379.
Guo, Y.J., Jetter, R., 2017. Comparative analyses of cuticular waxes on various organs of potato (Solanum tuberosum L.). J. Agric. Food Chem. 65 (19), 3926–3933.
Harholt, J., Moestrup, O., Ulvskov, P., 2016. Why plants were terrestrial from the beginning. Trends Plant Sci. 21 (2), 96–101.
Haslam, T.M., Mañas-Fernández, A., Zhao, L., Kunst, L., 2012. Arabidopsis ECERIFERUM2 is a component of the fatty acid elongation machinery required for fatty acid extension to exceptional lengths. Plant Physiol. 160 (3), 1164–1174.
Hauke, V., Schreiber, L., 1998. Ontogenetic and seasonal development of wax composition and cuticular transpiration of ivy (Hedera helix L.) sun and shade leaves. Planta 207 (1), 67–75.
Hosokawa, K., Fukunaga, Y., 1995. Production of essential oils by flowers of *Hyacinthus orientalis* l regenerated in-vitro. Plant Cell Rep. 14 (9), 575–579.
Hunsche, M., Noga, G., 2011. Cuticular wax load and surface wettability of leaves and fruits collected from sweet cherry (Prunus avium) trees grown under field conditions or inside a polytunnel. Acta Physiol. Plant. 33 (5), 1785–1792.
Il Hwang, D., Won, K.J., Kim, D.Y., Kim, B., Lee, H.M., 2017. Cinnamyl alcohol, the bioactive component of chestnut flower absolute, inhibits adipocyte differentiation in 3T3-L1 cells by downregulating adipogenic transcription factors. Am. J. Chin. Med. 45 (4), 833–846.
Jeffree, C., 2006. The fine structure of the plant cuticle. In: Riederer, M., Muller, C. (Eds.), Biology of the Plant Cuticle, pp. 11–144.
Jetter, R., Kunst, L., Samuels, A.L., 2006. Composition of plant cuticular waxes. In: Riederer, M., Muller, C. (Eds.), Biology of the Plant Cuticle. Blackwell Publishing Ltd, Oxford Uk, pp. 145–181.
Ji, X.F., Jetter, R., 2008. Very long chain alkylresorcinols accumulate in the intracuticular wax of rye (Secale cereale L.) leaves near the tissue surface. Phytochemistry 69 (5), 1197–1207.
Koch, K., Bennemann, M., Bohn, H.F., Albach, D.C., Barthlott, W., 2013. Surface microstructures of daisy florets (Asteraceae) and characterization of their anisotropic wetting. Bioinspiration Biomimetics 8 (3), 15.
Koch, K., Ensikat, H.-J., 2008. The hydrophobic coatings of plant surfaces: epicuticular wax crystals and their morphologies, crystallinity and molecular self-assembly. Micron 39 (7), 759–772.
Kosma, D.K., Bourdenx, B., Bernard, A., Parsons, E.P., Lu, S., Joubes, J., Jenks, M.A., 2009. The impact of water deficiency on leaf cuticle lipids of arabidopsis. Plant Physiol. 151 (4), 1918–1929.
Kosma, D.K., Rowland, O., 2016. Answering a four decade-old question on epicuticular wax biosynthesis. J. Exp. Bot. 67 (9), 2538–2540.
Kunst, L., Samuels, L., 2009. Plant cuticles shine: advances in wax biosynthesis and export. Curr. Opin. Plant Biol. 12 (6), 721–727.
Kuroda, K., 2000. Analytical pyrolysis products derived from cinnamyl alcohol-end groups in lignins. J. Anal. Appl. Pyrolysis 53 (2), 123–134.
Lee, S., Kim, H., Kim, R., Suh, M., 2014. Overexpression of Arabidopsis MYB96 confers drought resistance in *Camelina sativa* via cuticular wax accumulation. Plant Cell Rep. 33 (9), 1535–1546.
Lee, S.B., Suh, M.C., 2015. Advances in the understanding of cuticular waxes in Arabidopsis thaliana and crop species. Plant Cell Rep. 34 (4), 557.
Letizia, C.S., Cocchiara, J., Lalko, J., Lapczynski, A., Api, A.M., 2005. Fragrance material review on cinnamyl alcohol. Food Chem. Toxicol. 43 (6), 837–866.
Long, L.M., Patel, H.P., Cory, W.C., Stapleton, A.E., 2003. The maize epicuticular wax layer provides UV protection. Funct. Plant Biol. 30 (1), 75–81.
Luis, A., Domingues, F., Duarte, A.P., 2016. Biological properties of plant-derived alkylresorcinols: mini-review. Mini Rev. Med. Chem. 16 (11), 851–854.
Luna, Á., 2014. Biosynthesis and Accumulation of Very-Long-Chain Alkylresorcinols in Cuticular Waxes of *Secale Cereale* and *Brachypodium Distachyon* (T). Botany. University of British Columbia, Vancouver.
Ma, D.M., Xu, C., Alejos-Gonzalez, F., Wang, H., Yang, J.F., Judd, R., Xie, D.Y., 2018. Overexpression of Artemisia annua cinnamyl alcohol dehydrogenase increases lignin and coumarin and reduces artemisinin and other sesquiterpenes. Front. Plant Sci. 9, 12.
Marinho, C.R., Souza, C.D., Barros, T.C., Teixeira, S.P., 2014. Scent glands in legume flowers. Plant Biol. 16 (1), 215–226.
Ni, Y., Guo, Y.J., Han, L., Tang, H., Conyers, M., 2012. Leaf cuticular waxes and physiological parameters in alfalfa leaves as influenced by drought. Photosynthetica 50 (3), 458–466.
Niklasson, I.B., Delaine, T., Islam, M.N., Karlsson, R., Luthman, K., Karlberg, A.T., 2013. Cinnamyl alcohol oxidizes rapidly upon air exposure. Contact Dermatitis 68 (3), 129–138.
Palacios, C.E.J., Negri, G., Salatino, A., 2015. Esters and other constituents of the foliar cuticular wax of a soybean variety. Biochem. Syst. Ecol. 63, 198–200.
Pellmyr, O., 1992. Evolution of insect pollination and angiosperm diversification. Trends Ecol. Evol. 7 (2), 46–49.
Perera, M.A.D.N., Qin, W., Yandeau-Nelson, M., Fan, L., Dixon, P., Nikolau, B.J., 2010. Biological origins of normal-chain hydrocarbons: a pathway model based on cuticular wax analyses of maize silks: biological hydrocarbons. Plant J. 64 (4), 618–632.
Pichersky, E., Gershenzon, J., 2002. The formation and function of plant volatiles: perfumes for pollinator attraction and defense. Curr. Opin. Plant Biol. 5 (3), 237–243.
Pillonel, C., Mulder, M.M., Boon, J.J., Forster, B., Binder, A., 1991. Involvement of cinnamyl-alcohol dehydrogenase in the control of lignin formation in *Sorghum bicolor* moench. Planta 185 (4), 538–544.
Pino, J.A., Ferrer, A., Alvarez, D., Rosado, A., 1994. Volatiles of an alcoholic extract of flowers from plumeria rubra L. var. acutifolia. Flavour Fragrance J. 9 (6), 343–345.
Prato, T., Zeyuan, Q., Pederson, G., Fagre, D., Bengtson, L.E., Williams, J.R., 2010. Potential economic benefits of adapting agricultural production systems to future climate change. Environ. Manag. 45 (3), 577–589.
Purola, T., Lehtonen, H., Liu, X., Tao, F., Palosuo, T., 2018. Production of cereals in northern marginal areas: an integrated assessment of climate change impacts at the farm level. Agric. Syst. 162, 191–204.
Richardson, A., Franke, R., Kerstiens, G., Jarvis, M., Schreiber, L., Fricke, W., 2005. Cuticular wax deposition in growing barley (Hordeum vulgare) leaves commences in relation to the point of emergence of epidermal cells from the sheaths of older leaves. Planta 222 (3), 472–483.
Riederer, M., 1991. Cuticle as barrier between terrestrial plants and the atmosphere - significance of growth-structure for cuticular permeability. Naturwissenschaften 78 (5), 201–208.
Riederer, M., Schneider, G., 1989. Comparative-study of the composition of waxes extracted from isolated leaf cuticles and from whole leaves of citrus - evidence for selective extraction. Physiol. Plantarum 77 (3), 373–384.
Samuels, L., Kunst, L., Jetter, R., 2008. Sealing plant surfaces: cuticular wax formation by epiclermal cells. Annu. Rev. Plant Biol. 59, 683.

Sanchez, F.J., Manzanares, M., de Andres, E.F., Tenorio, J.L., Ayerbe, L., 2001. Residual transpiration rate, epicuticular wax load and leaf colour of pea plants in drought conditions. Influence on harvest index and canopy temperature. Eur. J. Agron. 15 (1), 57–70.

Tava, A., Pecetti, L., 1997. Volatiles from Medicago sativa complex flowers. Phytochemistry 45 (6), 1145–1148.

Verardo, G., Pagani, E., Geatti, P., Martinuzzi, P., 2003. A thorough study of the surface wax of apple fruits. Anal. Bioanal. Chem. 376 (5), 659–667.

Wang, Y., Wang, J., Chai, G., Li, C., Hu, Y., Chen, X., Wang, Z., 2015. Developmental changes in composition and morphology of cuticular waxes on leaves and spikes of glossy and glaucous wheat (*Triticum aestivum* L.). PLoS One 10 (10).

Webber, H., Gaiser, T., Ewert, F., 2014. What role can crop models play in supporting climate change adaptation decisions to enhance food security in Sub-Saharan Africa? Agric. Syst. 127, 161–177.

Westerkamp, C., 1997. Keel blossoms: bee flowers with adaptations against bees. Flora 192 (2), 125–132.

Whitney, H.M., Kolle, M., Andrew, P., Chittka, L., Steiner, U., Glover, B.J., 2009. Floral iridescence, produced by diffractive optics, acts as a cue for animal pollinators. Science 323 (5910), 130–133.

Wong, K.C., Teng, Y.E., 1994. Volatile components of *Mimusops elengi* L. flowers. J. Essent. Oil Res. 6 (5), 453–458.

Yang, G., Espelie, K.E., Todd, J.W., Culbreath, A.K., Pittman, R.N., Demski, J.W., 1993. Cuticular lipids from wild and cultivated peanuts and the relative resistance of these peanut species to fall armyworm and thrips. J. Agric. Food Chem. 41 (5), 814–818.

Yeats, T.H., Rose, J.K.C., 2013. The formation and function of plant cuticles. Plant Physiol. 163 (1), 5–20.

Yin, Y., Bi, Y., Chen, S., Li, Y., Li, Y., Wang, Y., Ge, Y., Ding, B., Zhang, Z., 2011. Chemical composition and antifungal activity of cuticular wax isolated from Asian pear fruit (cv. Pingguoli). Sci. Hortic. 129 (4), 577–582.